Short-range Forecasting Research

Forecasting Research Division
Technical Report No. 32

Bright band correlations for layered precipitation; the comparison of Chilbolton radar data and Hardaker model output

by
A G Davies

November 1992

Meteorological Office
London Road
Bracknell
Berkshire
RG12 2SZ
United Kingdom

Met.O.(FR) Technical Report No. 32

Bright band correlations for layered precipitation; the comparison of Chilbolton radar data and Hardaker model output.

by

A G Davies

November 1992

Met.O.(FR)
(Forecasting Research Division)
Meteorological Office
London Road
Bracknell
Berks, RG12 2SZ

Note

This paper has not been published. Permission to quote from it should be obtained from the Assistant Director of the above Meteorological Office Branch.

Bright-band parameter correlations for layered precipitation; the comparison of Chilbolton radar data and Hardaker model output.

Ashley Gerard Davies
Met O S (Precipitation Analysis Methods)
Meteorological Office, Bracknell, U.K.

25 th November 1992

Abstract

Vertical profiles of reflectivity measured by the Chilbolton radar which were representative of stratiform precipitation with an identifiable bright band feature were analysed to determine correlations between such parameters as bright band maximum reflectivity, background reflectivity (and therefore background rainfall) and bright band depth. These data were then compared with data from Hardaker's bright band model, with the intention of evaluating Hardaker's model for future inclusion in the radar analysis scheme. Analysis of the Chilbolton data showed high correlations between bright band intensity (maximum reflectivity) and the area of the bright band peak, and between bright band maximum reflectivity and underlying rainfall rate. The latter correlation confirms a major assumption of Hardaker's model. These relationships could be used to correct for the bright band in stratiform precipitation conditions. However, Hardaker's model overestimates bright band intensity, even after allowances were made for the resolution limitations of the Chilbolton data and model output. Further work is necessary on the modelling of the melting layer in Hardaker's model.

Introduction

The purpose of this study was primarily to compare a bright band model developed by Paul Hardaker at the University of Essex (Department of Mathematics) with data from actual radar observations, and so evaluate the model. This bright band model (henceforth referred to as the Hardaker model) is either to be applied to bright band correction of network radar data directly or be used as a research tool to aid development of correction techniques. A key prediction of the model is that the bright band intensity is a function of the underlying rainfall rate, implying that there is information on the true rainfall rate in the bright band region. The model output was compared with actual radar data from the S-band (10 cm) experimental radar at Chilbolton.

Work on the comparison of averaged reflectivity-height profiles derived from the radars at Chenies and Chilbolton (Davies, 1992a) demonstrated the variability of the bright band structure. Following

this study a new method of correcting the radar data on a pixel-by-pixel basis was proposed (Kitchen, 1992). The proposed correction method initially assumed a relationship between the bright band intensity and the underlying rainfall rate, based on the Hardaker model.

The second part of this study was to arrive at an appropriate parameterization of the reflectivity profile in the bright band for use in the correction scheme. To achieve this, the correlations between bright band maximum reflectivity, the reflectivity in the ice (that is, above the bright band), the reflectivity in the rain (below the bright band), the area of bright band peak above the background rainfall reflectivity and the depth of the bright band were studied. A high correlation would be necessary to warrant inclusion in any resulting correction scheme.

1 Data selection

Previously, correlations between inferred bright band maximum reflectivity height and surface temperature were determined for different types of precipitation, frontal and convective (Davies, 1992b). That study showed a strong correlation between surface temperature and freezing level for stratiform rainfall, assuming that the inferred lapse rate between surface and freezing level was constant.

The same rigorous profile selection procedure developed for the maximum reflectivity/surface temperature study was used in this study. For a reflectivity-height profile from the Chilbolton data set to be selected, it had to satisfy a number of criteria. A full description of the selection procedure is given in Davies (1992b), but it is sufficient to say that profiles were initially selected on the basis of the minimum height of the level of maximum reflectivity, that the maximum reflectivity was above a set threshold, that the precipitation type was correct for the case study, that a definite peak existed, and that the inferred height of the bright band was within limits set by maximum and minimum possible lapse rates. Only vertical reflectivity profiles with a single bright band peak were selected. Of 18841 Chilbolton profiles, 2080 profiles were accepted as representing stratiform rain.

This case study is limited to the analysis of profiles of stratiform precipitation, the type of precipitation most common in Britain. Although many convective features exhibit a bright band over part of their area, there is often too much variation in profile shapes to make quick analysis of RHIs possible.

2 Comparison of theoretical data with observed data.

2.1 Hardaker's model

Hardaker's model is based upon the model of Dissanayake (1978). Dissanayake's model assumes that there is a continuous supply of aggregate snowflakes, modelled as two-layer spheres with a water shell and an ice core. The snowflakes fall at their terminal velocity. It is assumed that there is a one-to-one correspondence between the snowflake, before melting, and the raindrop, after melting, with the drops conforming to a Marshall-Palmer drop size distribution. The one-to-one correspondence implies that no aggregation, break-up or drop shedding occurs.

Changes to Dissanayake's model were made by Hardaker and Holt (1992) (see also Hardaker et. al., 1992) to make the model practically useful, allowing for atmospheres that are sub-saturated,

as variations in relative humidity affected the way in which snowflakes melted. Mie scattering was assumed throughout the model when calculating the backscatter cross-section of individual melting particles. A further extension to Dissanayake's model was to allow for propagation effects through the rainfall and up to the base of the melting layer.

2.2 Hardaker's model and the proposed correction scheme

Use of Hardaker's model would be preferable over fitting Chilbolton observations because (i) the model predicts different bright band intensities for S-band and C-band radars; (ii) the model would be the easiest option to implement, and (iii) there are uncertainties in the Chilbolton data due to an average 5 km limit of resolution.

The correction scheme requires that the reflectivity profile in the melting layer is specified and any variability in the shape or intensity is related to available parameters, either measured or inferred. Hardaker's model predicts the shape of the profile given a number of variables (including the temperature and humidity profiles, and background rainfall rate). Background rainfall rate seems to be the most important of these variables.

2.3 Questions regarding Hardaker's model

The important areas of comparison between Hardaker's model output and actual radar data are as follows.

1. Does the bright band intensity increase with underlying rain rate as implied by Hardaker's model ?
2. Does the Hardaker model predict a realistic bright band intensity ?
3. Does the Hardaker model predict a realistic bright band depth ? Hardaker's model predicts that the bright band depth is virtually constant for a fixed lapse rate.

3 Chilbolton reflectivity profiles

The Chilbolton radar is a 10 cm wavelength, high resolution research radar operated by the Rutherford-Appleton laboratory. The beam is 0.25^0 wide and the resolution in range is 300 m. The radar executed series of 3 RHI scans along three azimuths, each scan being constructed from elevation increments of 0.25^0 up to 15^0. Reflectivity profiles were produced for three ranges along three azimuths by averaging data within 200 m deep height bands along a 5.4 km line (Davies, 1992a). A full description of how the radar data is processed is given in Kitchen and Brown (1992), but to summarise, basic data from the Chilbolton radar were produced by averaging the absolute magnitude of the received signals; reflectivity values were transformed into an equivalent rainfall rate, grouped together according to range and height bins to emulate 5 x 5 km pixels, and the average reflectivity for the 'pixel' computed.

The Chilbolton profiles are constructed from data points starting from 300 meters above the ground and ascending in $\approx$ 200 m increments. Figure 1 shows a typical reflectivity-height profile.

The maximum reflectivity is at a height of 1299 m, and the background value and area of the bright band are shown. Background and area are defined below.

4 Definition of terms

4.1 Background reflectivity

The background reflectivity was taken to be the smallest reflectivity of three levels beneath the bright band maxima level, at maxima level - 400 m, maxima level - 600 m and maxima level - 800 m. As the half width of the bright band is always less than $\approx$ 600 m, this ensured that a level that was not part of the actual bright band was always chosen.

This reflectivity value (Z) is empirically converted into an equivalent rainfall rate (R), using the relationship

$$Z = 200R^{1.6} \tag{1}$$

where Z is in $mm^6\ m^{-3}$ and R is in $mm\ h^{-1}$. This reflectivity value is taken to be the reflectivity of the rain beneath the bright band, that is, the background rainfall, which if not for low level growth (or other enhancement of rainfall rate) or evaporation (or other reduction of rainfall rate), would be the surface rainfall. This was in line with Hardaker's model.

4.2 Bright band depth

The depth of the bright band, after some trial and error, was finally defined as the distance between the intercept of the background reflectivity and the 'arms' of the top and bottom of the bright band peak feature (see figure 1), and extrapolating or interpolating between profile data points whenever necessary. This was acceptable where the peak was triangular, and could be defined by two segments. Where there were more than two profile segments making up the peak, for example, where the peak is truncated, the two profile segments above the chosen maximum reflectivity were compared with each other, as were the two segments below the maxima. The longest segment of the two was chosen as the 'arm'. If the segments were the same length, the segment with the shallowest angle to the horizontal was selected (see figure 1). This very conservative method of calculating bright band depth was necessary due to the vertical resolution of the Chilbolton data, which is actually better than the resolution obtained from most radars in the UK Weather Radar Network at present.

4.3 Bright band area

The area of the bright band peak was taken to be the area of the profile between maximum reflectivity value and the background reflectivity (see figure 1). Where the reflectivity above the bright band peak was greater then the background reflectivity, the part of the RHI profile making up the upper boundary of the bright band peak was extended until it intercepted the background reflectivity. Having determined the limits of the bright band peak, calculating the area is a trivial matter, the peak being constructed from a number of quadrilaterals and triangles.

4.4 Resolution problems

4.4.1 Chilbolton data

The accurate determination of bright band depth, maximum reflectivity and bright band peak area is limited by the 200 m vertical resolution of the Chilbolton profiles. This sometimes has the effect of truncating the peak, and heavily weights the measurement of bright band depth towards the 200 m height increments. As the bright band is of the order of $\approx$ 500 m deep, depths calculated directly from the Chilbolton profiles are unlikely to be accurate, and therefore of little use in any parametrisation scheme involving individual RHIs. This resolution problem will hopefully be overcome by using the area of the bright band peak as opposed to depth of bright band.

4.4.2 Hardaker's model output

The vertical resolution of Hardaker's model output is 50 m. The model shows little variation in the depth of the bright band at the background level regardless of maximum reflectivity value and surface rainfall rate, but even so, the limit of resolution affects the depth calculation. Hardaker's model output is summarised in table 1, which shows surface rainfall rate and equivalent background reflectivity (the reflectivity in the rain), maximum reflectivity in the bright band, reflectivity in the ice and the area of the bright band peak.

Hardaker's model output did show a slight increase in the depth of the bright band with increasing maximum reflectivity. However, when the depth of the bright band was calculated using the same method used on the Chilbolton profiles, the bright band seemed to narrow as maximum reflectivity increased, calculated depths ranging from 399 m to 283 m. The reason why the bright band seemed to be getting shallower as rainfall increased was due to the conservative methodology adopted, using extrapolation back to the background level of the 'arms' of the bright band from the maximum reflectivity point or points of truncation of the peak. As the maxima increased, the angle at the apex of the peak decreased, and so did the base of the peak triangle, the bright band depth. The calculated depth decreased at a faster rate than the model depth increased, as surface rainfall increased.

5 Bright band intensity and background reflectivity.

The relationship between bright band intensity and background reflectivity lies at the heart of Hardaker's model, and therefore at the heart of the bright band correction method. Figure 2 shows a plot of background reflectivity against maximum reflectivity for 1524 Chilbolton profiles, and the equivalent data from Hardaker's model. The Chilbolton profiles used to produce figure 2 have undergone a slightly different selection procedure from that described in section 1. All profiles with a bright band maximum reflectivity level under 1500 m have been discarded, and the threshold for maximum reflectivity has been reduced from 1000 $mm^6\ m^{-3}$ to 300 $mm^6\ m^{-3}$. The dotted line parallel to the Hardaker line is also Hardaker's data, but with the maximum reflectivity value reduced by 36 %, in an attempt to match the truncation of the Chilbolton data caused by a poor vertical resolution. This estimate was based upon a two-stage calculation. First, the Chilbolton beam power profile was convoluted with a reflectivity profile from the Hardaker model, which allows

for the effect of the finite Chilbolton beam width. In the absence of any information on the shape of the Chilbolton beam profile, the same function was used as was fitted to the observed power profile of the operational radars, but using a quarter-degree beam width. The resultant reflectivity profiles were then averaged over 200 m in the vertical and 5 km in the horizontal, in the same way that the actual Chilbolton profiles were constructed. The bright band peak was placed at various position on the beam and the resultant percentage reduction in peak intensity averaged.

It is obvious that Hardaker's model is over-estimating the bright band maximum reflectivity for background reflectivities above 20 dBZ.

The correlation between bright band intensity and underlying rainfall was high, 0.884, implying a link between bright band intensity and background rainfall rate that warranted further investigation. To see what happens at low maximum reflectivities, the maximum reflectivity threshold (THOLD) was removed, and all profiles satisfying the other selection criteria were added, down to a minimum acceptable background reflectivity of 0.1 dBZ ($\approx$ 1 mm^6 m^{-3}). The 1500 m base for levels of maximum intensity was retained. The results are shown in figure 3. In total, 2200 profiles passing the selection procedure. The correlation increased to 0.937, implying a very strong relationship between bright band intensity and underlying rainfall. The spread of data at very low background reflectivities is partially due to less well defined bright bands, and in some cases there was difficulty in deciding if a peak was indeed a bright band feature. The result was, inevitably, a slight degradation in the quality of the data.

Hardaker's model output for background reflectivity below $\approx$ 18 dBZ compared very well with the additional data. The slight kink in the model output at background = 14 dBZ is not seen in the actual data, although the increased scattering of data in this region would make this difficult to see.

6 Reflectivity(ice) compared with reflectivity(rain)

Figure 4 shows reflectivities in the ice, in the region above the bright band, and reflectivities in the rain, beneath the bright band. Data from Chilbolton, Hardaker, and the Heymsfield (1977) observations are shown (Heymsfield fitted regression relationships to an extensive range of aircraft-based and radar observations). For clarity, the regression line and the Hardaker and Heymsfield data are shown in figure 5. The Hardaker data is almost identical to that from Heymsfield, and also is close to the Chilbolton data. The implication from this is that the overestimation of maximum reflectivity by Hardaker's model is not in the basic micro-physical assumptions relating the snow size distribution at the top of the melting layer to the underlying rainfall rate. It appears to be a problem in the melting region, most probably in the scattering calculation.

7 Relationship between area and background and maximum reflectivities.

Because the 200 m resolution of the vertical reflectivity profile has the effect of truncating the bright band peak and increasing the bright band depth, the most stable parameter to use in the profile parametrization may be the bright band area. Unpublished work by R. Brown (U.K. Met. Office)

showed that the area of the bright band was less affected by the imposed Chilbolton resolution than the bright band depth. The simulation of the averaging present in the Chilbolton profiles was also used to investigate the effect on the area under the bright-band peak. It was found that this was conserved to within about 12 %.

Figure 6 shows the relationship between the $\log_{10}$ (bright band maximum-background reflectivity), and the area of the bright band for the Chilbolton data, as well as the data from Hardaker's model. Once again, the overestimation of the bright band maximum by Hardaker causes the divergence seen above rainfall rates of 1.0 mm h^{-1}. The correlation for the Chilbolton data, 0.986, is very high, one obvious reason being that the area is a function of the size of the peak. This correlation, and the implied link between area and bright band maximum reflectivity, is the best tool for deriving a correction scheme for operational radar data.

Because the slope of the best fit regression line is greater than 1, this infers that the depth of the bright band increases with peak intensity, given that the bright band peak is triangular. Bright band depth is discussed below. Figure 7 shows area of the bright band peak against background reflectivity, comparing the Chilbolton and Hardaker data. The slopes of the two data sets are similar, but the areas of the Hardaker data are too large, due to maxima overestimation. The correlation for the Chilbolton area is 0.759, which is probably not high enough to use in a correction scheme.

8 Relationship between depth and area

Figure 8 shows the depth of the bright band and the area of the bright band, and figure 9 shows the area of the bright band calculated assuming that the bright band is triangular: the peak area is calculated using the best fit regression line in figure 6, using the maximum and background reflectivities. Figures 8 and 9 show a rough trend that suggests that the bright band depth increases with area of peak, at a greater rate than the Hardaker model. However, the 200 m vertical resolution limit with the Chilbolton data may be an influencing factor.

9 Proposed correction scheme

The best option would be to use the observed bright band area and the bright band maximum intensity. Assuming a triangular bright band shape, the depth increases from 450 m at low rainfall rates (this figure was determined using the limited Chilbolton resolution) to 670 m at the highest rainfall rates. (Hardaker's model produces depths of 500 m to 550 m, for a lapse rate of 6 C km^{-1}. Using the conservative calculation method the depths range from 399 m to 283 m.) It is likely that future work will include a re-evaluation of this method of determining bright band depth.

The strategy for determining bright band depth prior to correcting data would be as follows:

1. Set underlying rainfall rate (background rate).
2. Determine bright band maximum reflectivity, from correlation between background and maximum reflectivities (correlation = 0.937, see figure 3).
3. Determine bright band area, using correlation between maximum-background reflectivity and area (correlation = 0.986, see figure 6).

4. The bright band depth is defined by the area, assuming the bright band is triangular.

10 Conclusions

1. A very high correlation was also found between $\log_{10}$ bright band maximum intensity and $\log_{10}$ background reflectivity (underlying rainfall rate), confirming a major assumption of Hardaker's model.

2. The Hardaker model overestimates bright band maximum reflectivity for a given background rainfall rate.

3. Hardaker's model agrees well with the Chilbolton data when reflectivities in the ice and rain are compared: this implies that the problem with lies in the modelling of the melting layer.

4. From the analysis of the Chilbolton data, a high correlation was found between $\log_{10}$ bright band maximum reflectivity and $\log_{10}$ bright band peak area. The strategy for determining bright band depth in a correction scheme is described above.

5. The Hardaker model does not show a significant increase in bright band depth with increasing bright band intensity. Such an increase is inferred from the Chilbolton data, but difficulty in defining bright band depth due to poor vertical resolution means any comparisons will be inaccurate. A major reason for the near-constant bright band depth in the model is that all the results were obtained for a constant lapse rate of 6 C km^{-1}. If the model lapse rate was reduced, the bright band depth should increase. Since heavier precipitation tends to be associated with a reduction in lapse rate in the bright band region, if the model was run with a reduced lapse rate at higher rainfall rates, a greater variety of bright band depths would occur.

6. Because the model overestimates bright band intensity at S-band, it is uncertain if the model can be trusted when adjusted to C-band. Further work is necessary on the melting layer in Hardaker's model.

7. The Hardaker model shows considerable merit and with further development should be acceptable for application to bright band corrections. Possibly, the peak overestimation is due to a fixed lapse rate, appropriate only for light rain.

11 References

Davies A.G. (1992a) — Evaluation of Koistinen's method of radar range and bright band correction. Unpublished Short Range Forecasting Division Technical Report no. 27, U.K. Meteorological Office.

Davies A.G. (1992b) — Relationship between surface temperature and the height of freezing layer. Unpublished Short Range Forecasting Division Technical Report. U.K. Meteorological Office. In preparation.

Dissanayake, A.W. (1978) — Cross-polarisation on satellite-Earth radio links. PhD thesis. Postgraduate School of Studies in Electrical and Electronic Engineering, University of Bradford, BD7 1DP, U.K.

Hardaker P.J., Holt A.R. and Collier C.G. (1992) — A theoretical study of scattering effects caused by the melting layer. 25th Inter. Conf. on Radar Meteorology. pp 725-732.

Hardaker P.J. and Holt A.R. (1992) — A study of experimental and theoretical vertical reflectivity profiles at X-band. Dept. of Math., Univ. of Essex Internal Report.

Heymsfield A.J. (1977) — Precipitation development in stratiform ice clouds: a microphysical and dynamical study. *J. Atmos. Sci.*, **34**, 367-381.

12 Tables and Figures

List of Tables

1. Hardaker's model output, showing surface rainfall rate and equivalent background reflectivity, the reflectivity in the rain, maximum reflectivity in the bright band, reflectivity in the ice and the area of the bright band peak.

List of figures

1. Example of vertical reflectivity profile, showing maximum reflectivity, peak area, background level and physical structure.

2. Background reflectivity (dBZ) against maximum reflectivity (dBZ). Figure shows Chilbolton data compared with Hardaker's model data, as well as Hardaker's model data using 64 % of maximum reflectivity to try and reduce maximum reflectivity overestimation. Axis also show equivalent rainfall rates. Hardaker's model tends to overestimate maximum reflectivity for a given background reflectivity.

3. Background reflectivity (dBZ) against maximum reflectivity (dBZ), with no threshold limit. The correlation, 0.937, is very high, implying a direct link between bright band intensity and underlying rainfall.

4. Rain (background) reflectivity (dBZ) against ice reflectivity (dBZ). Shows data for Chilbolton profiles with maxima above 700 m. For comparison with Hardaker's model output, see figure 5.

5. Rain (background) reflectivity (dBZ) against ice reflectivity (dBZ). Using the data in figure 4, the least-squares best fit regression line is calculated. Data from the Hardaker and Heymsfield model are shown here.

6. $\log_{10}$ (maximum reflectivity - background reflectivity) against $\log_{10}$ area of bright band above background. Figure shows Chilbolton data and the best-fit regression line.

7. Background reflectivity (dBZ) against $\log_{10}$ area of bright band peak above background value. 2079 Chilbolton points used, with a correlation of 0.748. Also, background reflectivity (dBZ) against $\log_{10}$ area of bright band peak for Hardaker's model data.

8. Depth of bright band against $\log_{10}$ area of bright band, from program calculation of area.

9. Depth of bright band against $\log_{10}$ area of bright band, assuming peak is triangular.

Table 1.

Hardaker's model output for S band radar.

Surface rainfall ($mm\ h^{-1}$)	Maximum reflect. (dB)	Maximum reflect. ($mm^6\ m^{-3}$)	Max Ze as rainfall rate ($mm\ h^{-1}$)	Ze(ice) ($mm^6\ m^{-3}$)	Ze(rain) ($mm^6\ m^{-3}$)	$\log_{10}$ Area of peak
0.1	17.26548	53.3	0.44	5.533	9.836	3.957
0.2	23.40738	219.1	1.06	10.273	14.413	4.640
0.3	27.54597	568.3	1.92	13.038	17.020	5.020
0.4	30.53995	1132.4	2.96	15.016	18.852	5.304
0.5	32.87166	1937.2	4.13	16.563	20.267	5.527
0.6	34.77208	3000.6	5.43	17.837	21.422	5.709
0.7	36.37012	4335.2	6.84	18.922	22.397	5.864
0.8	37.74499	5949.8	8.34	19.867	23.242	5.997
0.9	38.94872	7850.1	9.91	20.704	23.987	6.114
1.0	40.01731	10039.9	11.56	21.455	24.654	6.128
1.5	44.04406	25375.0	20.64	24.367	27.220	6.613
2.0	46.80639	47933.5	30.71	26.444	29.043	6.886
2.5	48.88929	77433.5	41.44	28.057	30.456	7.093
3.0	50.55072	113520.0	52.64	29.327	31.611	7.258
3.5	51.92652	155830.3	64.16	30.482	32.587	7.396
4.0	53.09666	204016.8	75.93	31.440	33.433	7.514
4.5	54.11207	257754.9	87.87	32.283	34.178	7.616
5.0	55.00709	316744.5	99.95	33.034	34.843	7.707
5.5	55.80594	380709.9	112.13	33.710	35.445	7.787
6.0	56.52630	449397.4	124.38	34.326	35.994	7.861
6.5	57.18148	522573.8	136.68	34.891	36.499	7.927
7.0	57.78169	600024.2	149.01	35.411	36.966	7.988

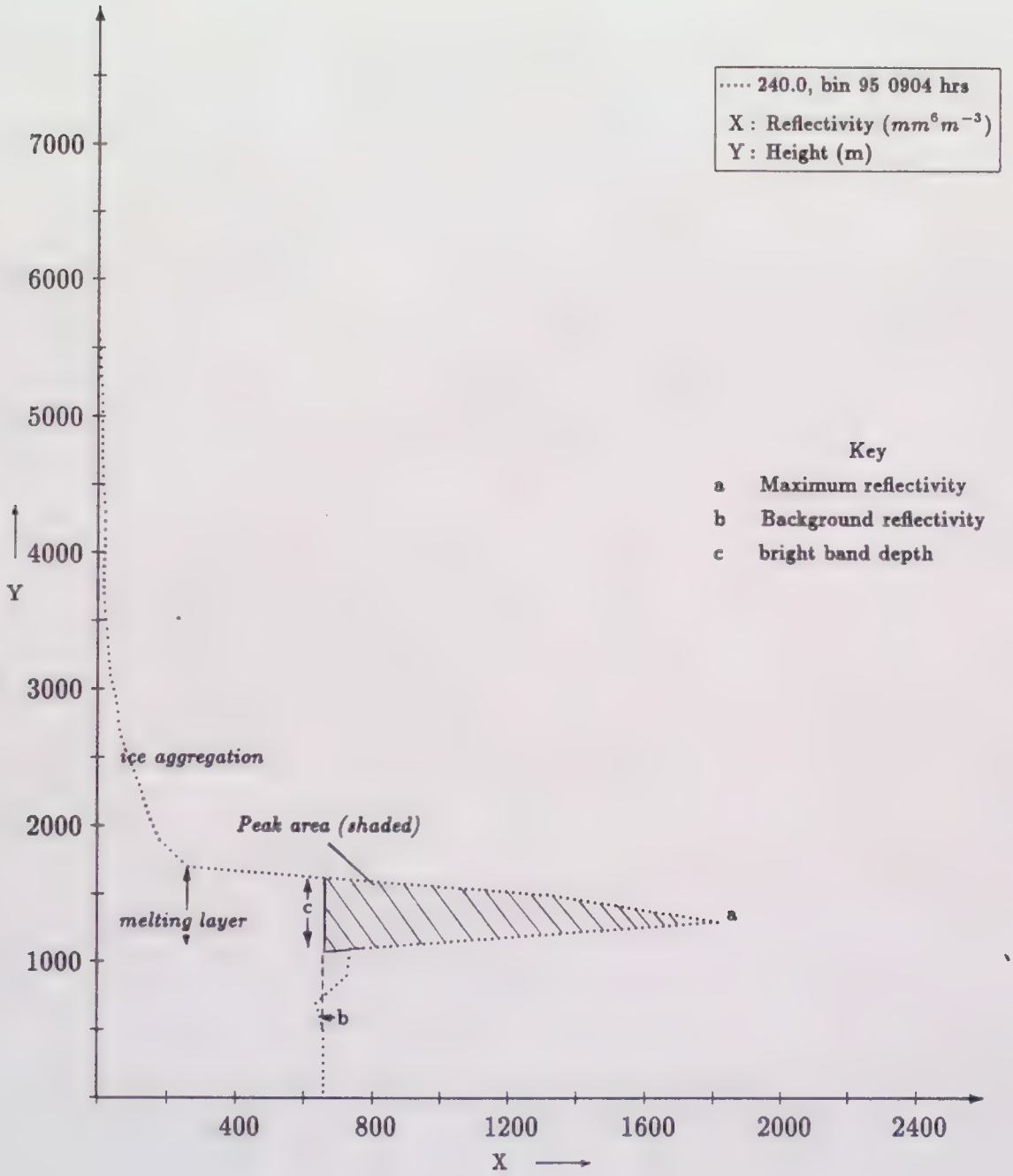

Figure 1

RHI showing typical bright band feature.
Chilbolton reflectivity data from 11/04/89

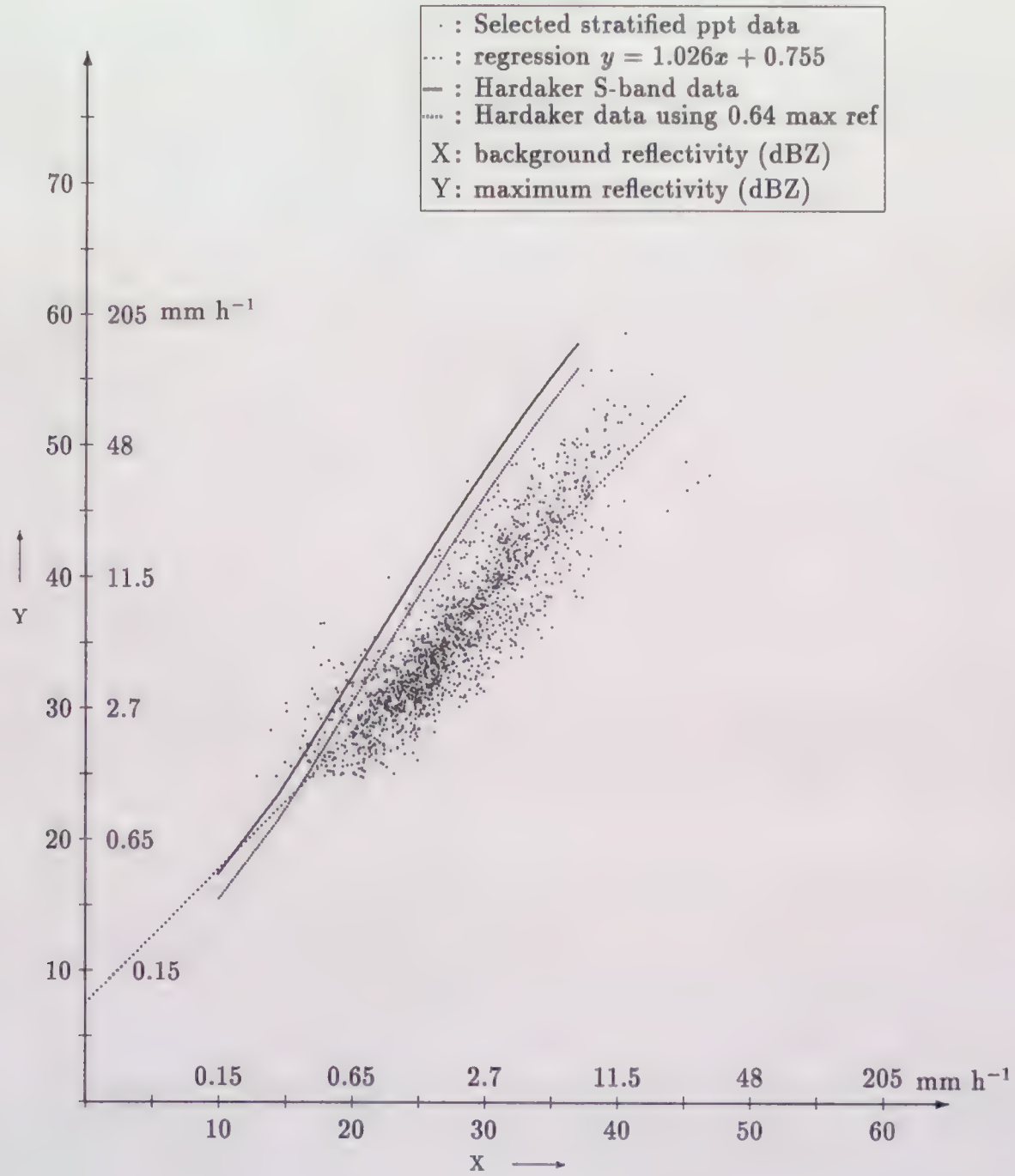

Figure 2

1524 Chilbolton profiles, maximum reflectivity level $\geq$ 1500 m.
Reflectivity threshold (THOLD) = 12.9 dBZ (300 mm^6 m^{-3}); correlation = 0.884.

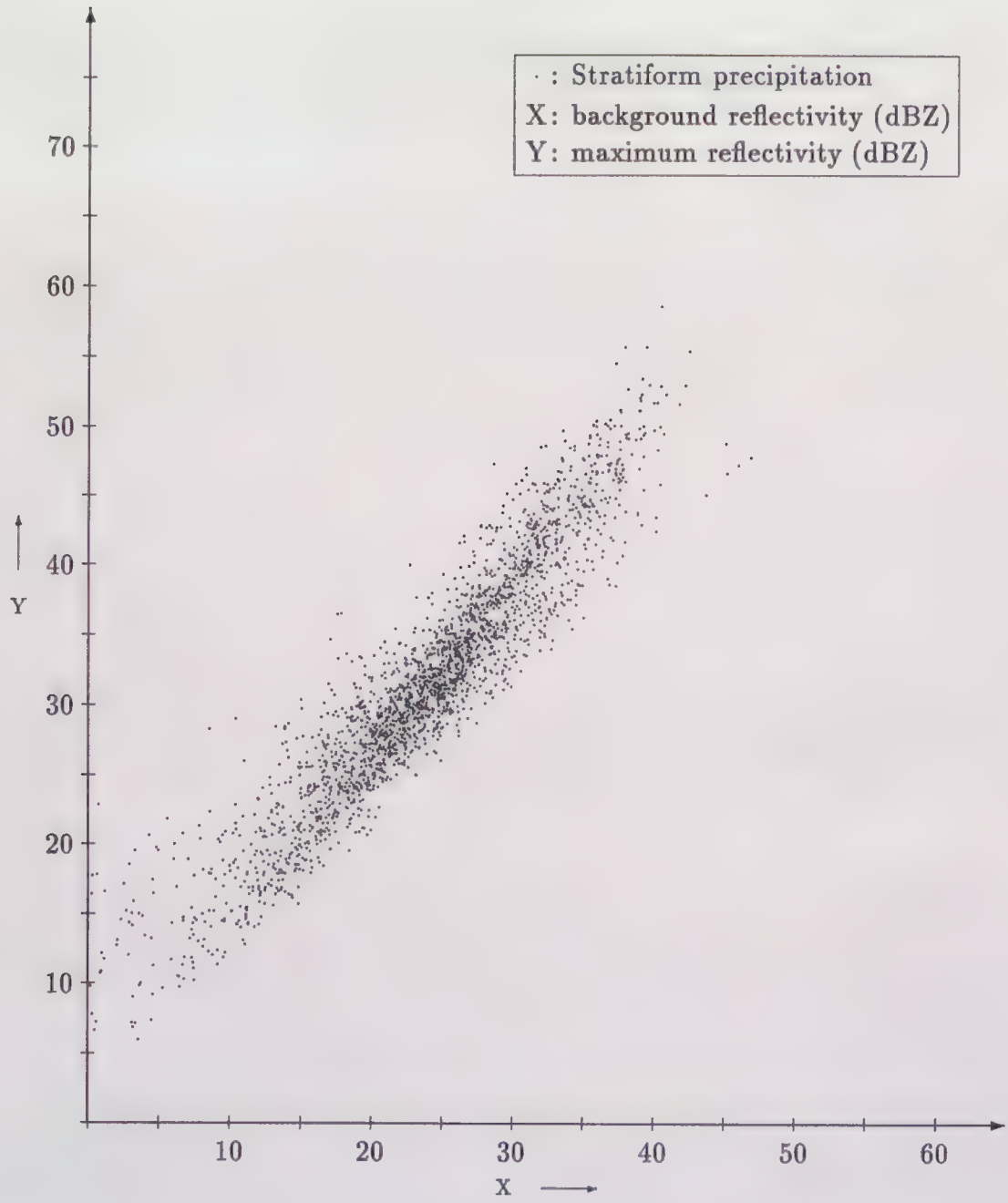

Figure 3

Chilbolton stratiform precipitation data. Minimum background reflectivity = 1.0 mm^6 m^{-3}. No maximum reflectivity threshold (THOLD) used. All maxima heights are above 1500 m. 2200 points used. Correlation = 0.937. Best fit least-squares regression line: $y = 1.045x + 0.671$

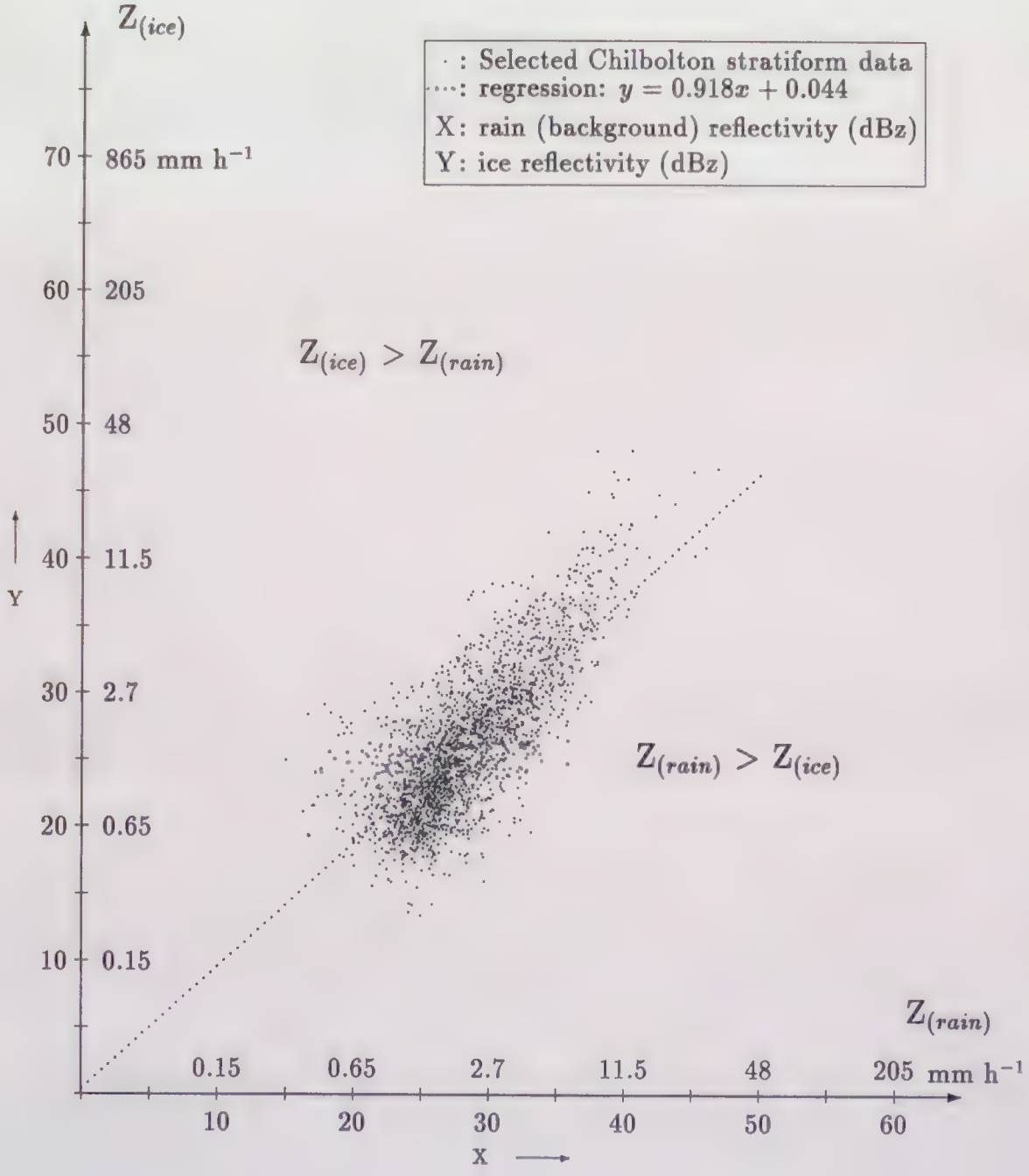

Figure 4

Reflectivity(rain) compared with reflectivity(ice).
Corr = 0.764, 2023 profiles used.

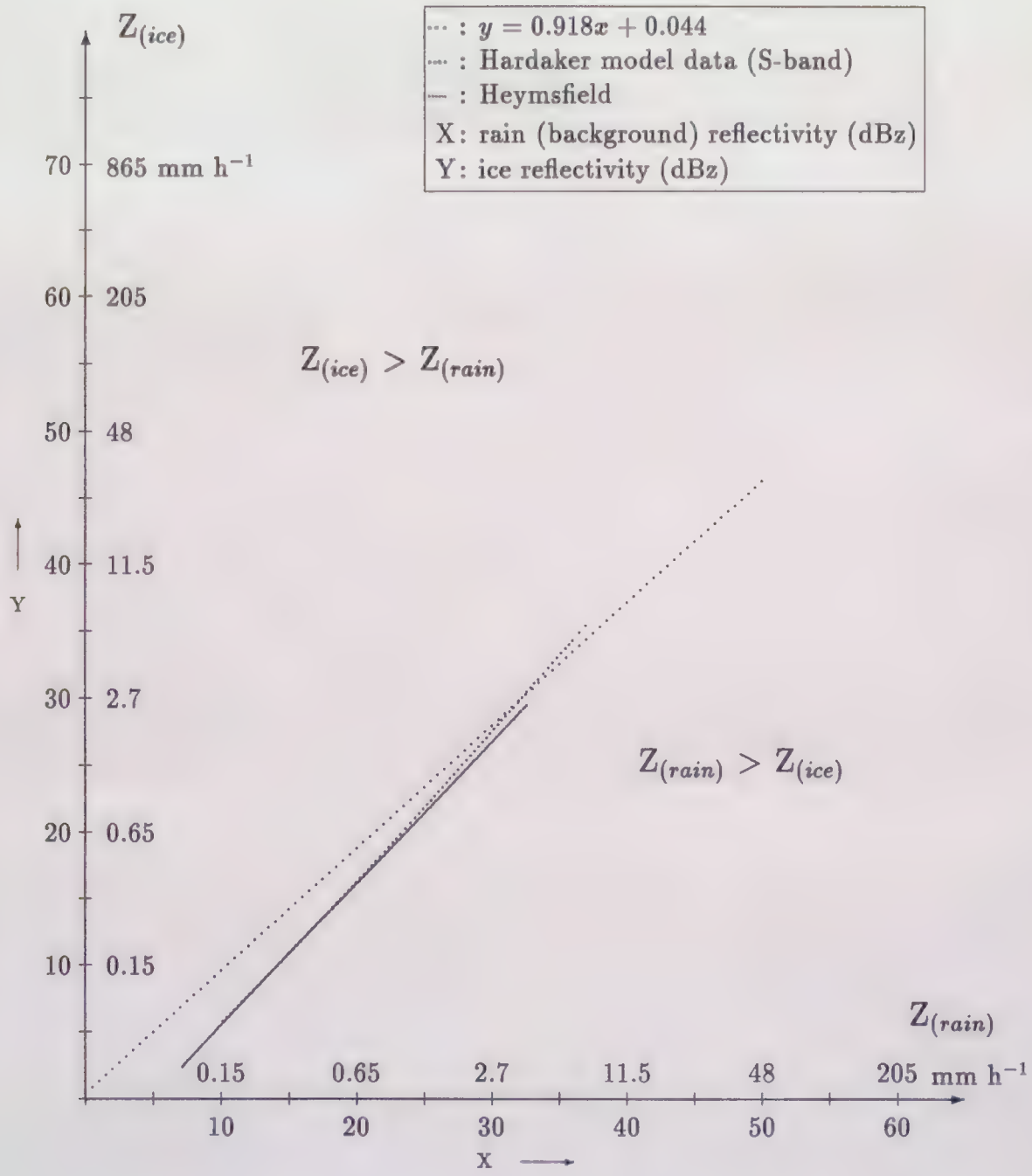

Figure 5

Comparison of curves for profiles with maximum reflectivity above 700 m. Correlation = 0.764, 2023 profiles used.

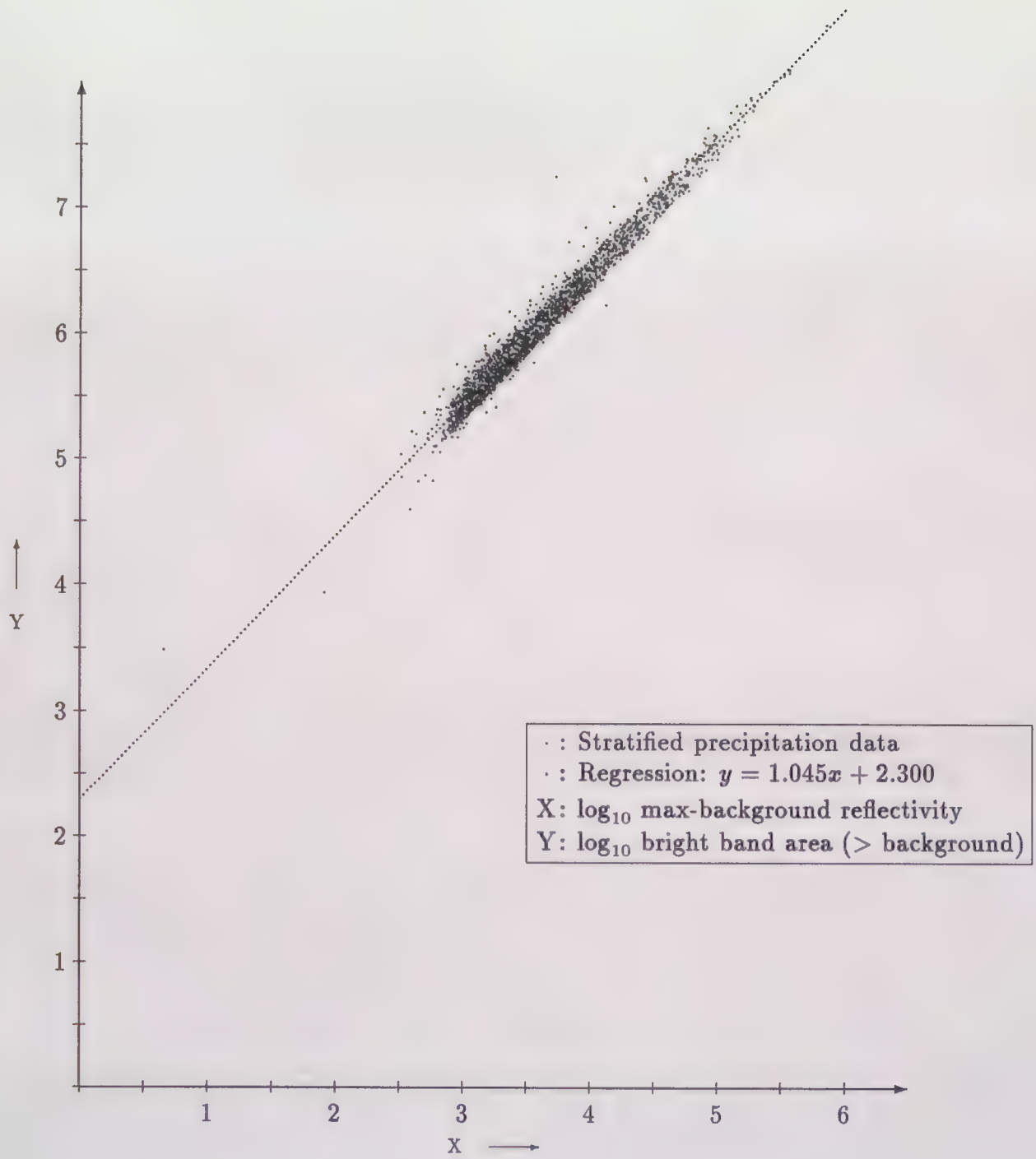

Figure 6

2080 Chilbolton profiles used. Correlation coefficient = 0.986

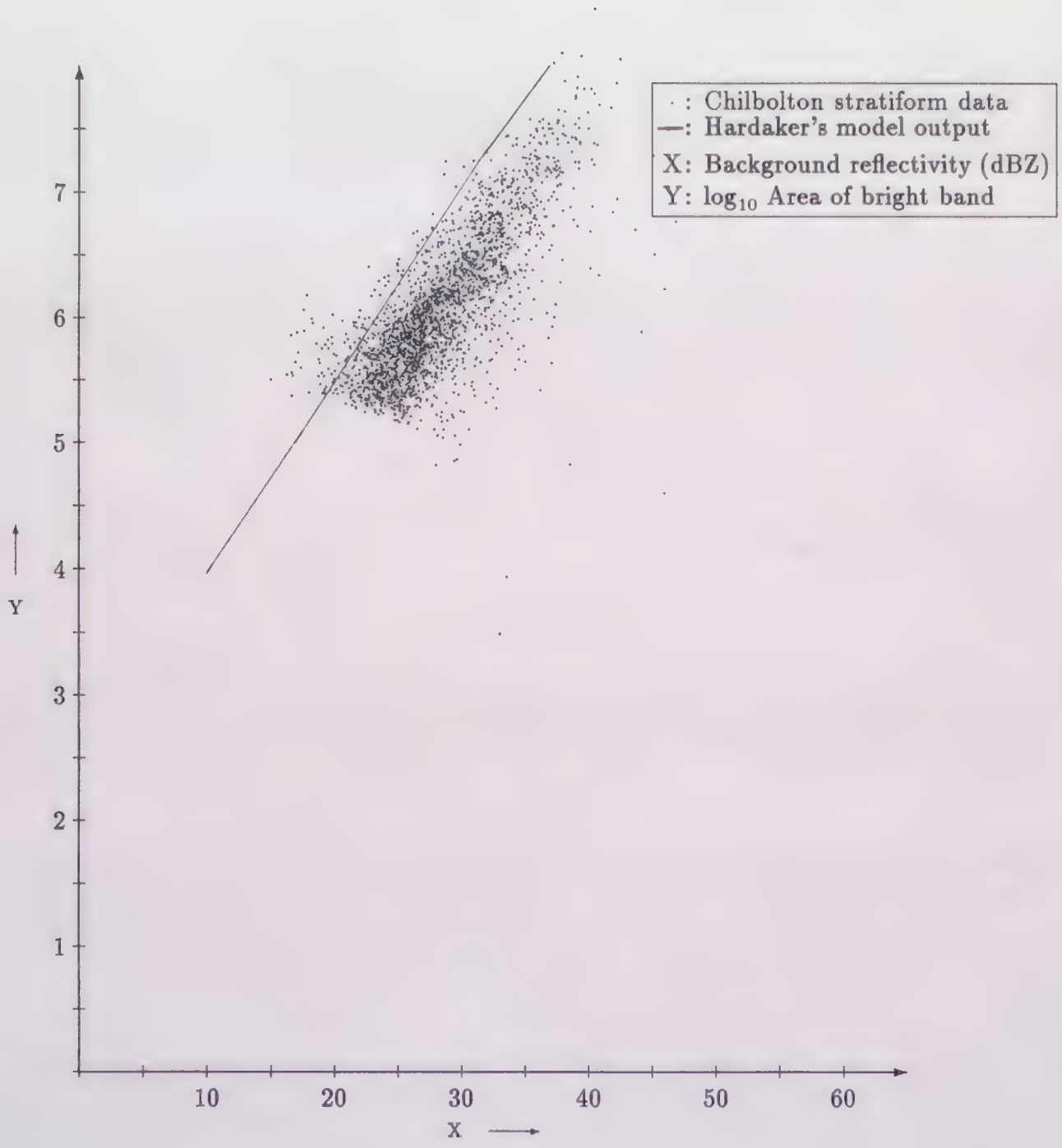

Figure 7

Comparison of Chilbolton data and Hardaker's model output. 2079 profiles used. Correlation coefficient = 0.748; regression line for Chilbolton data $y = 0.936x + 3.425$

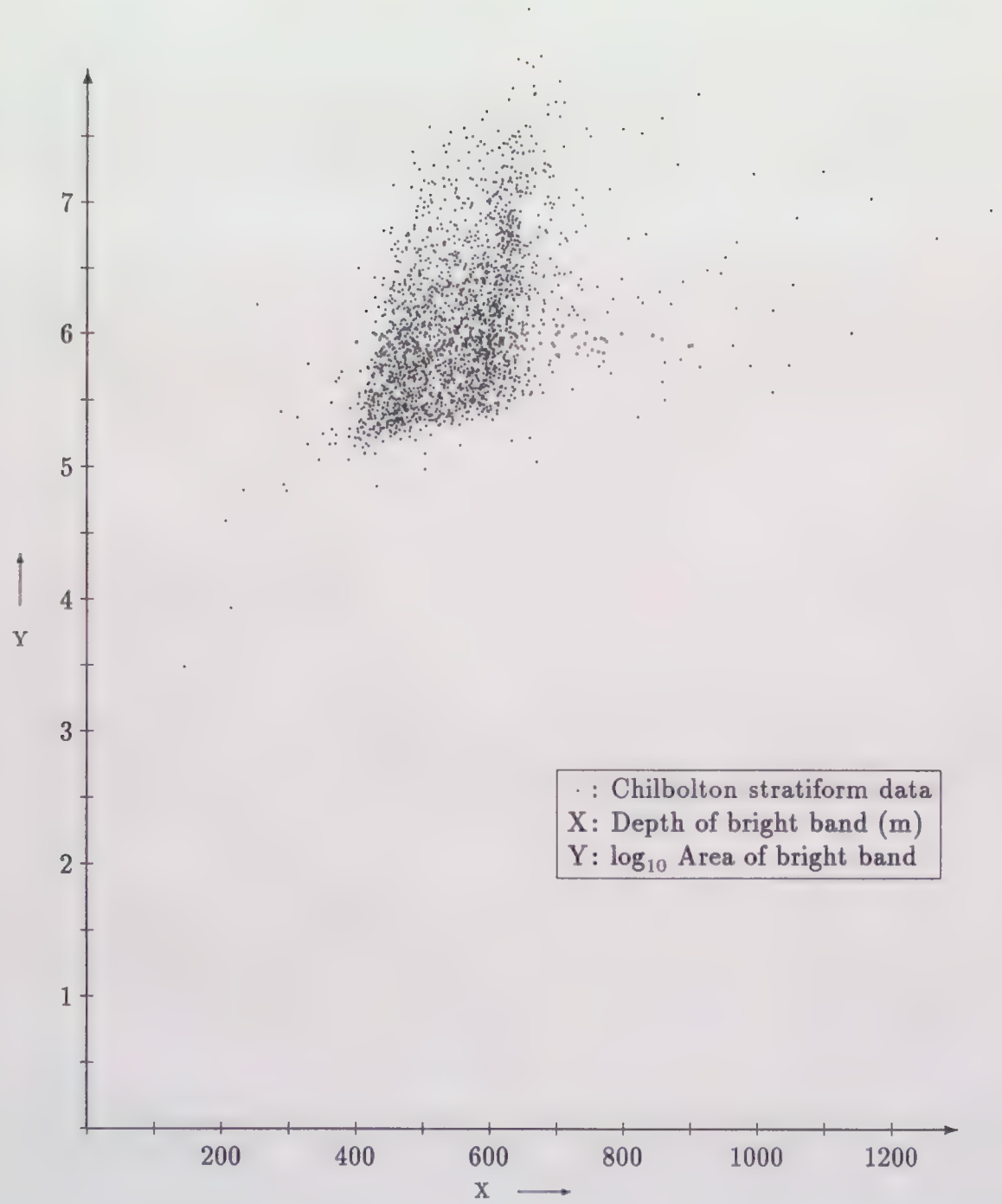

Figure 8

Calculation of bright band depth uses extrapolation/interpolation of RHI profile segments to background reflectivity level. 2079 profiles used (max ref THOLD = 1000 mm^6 m^{-3}).

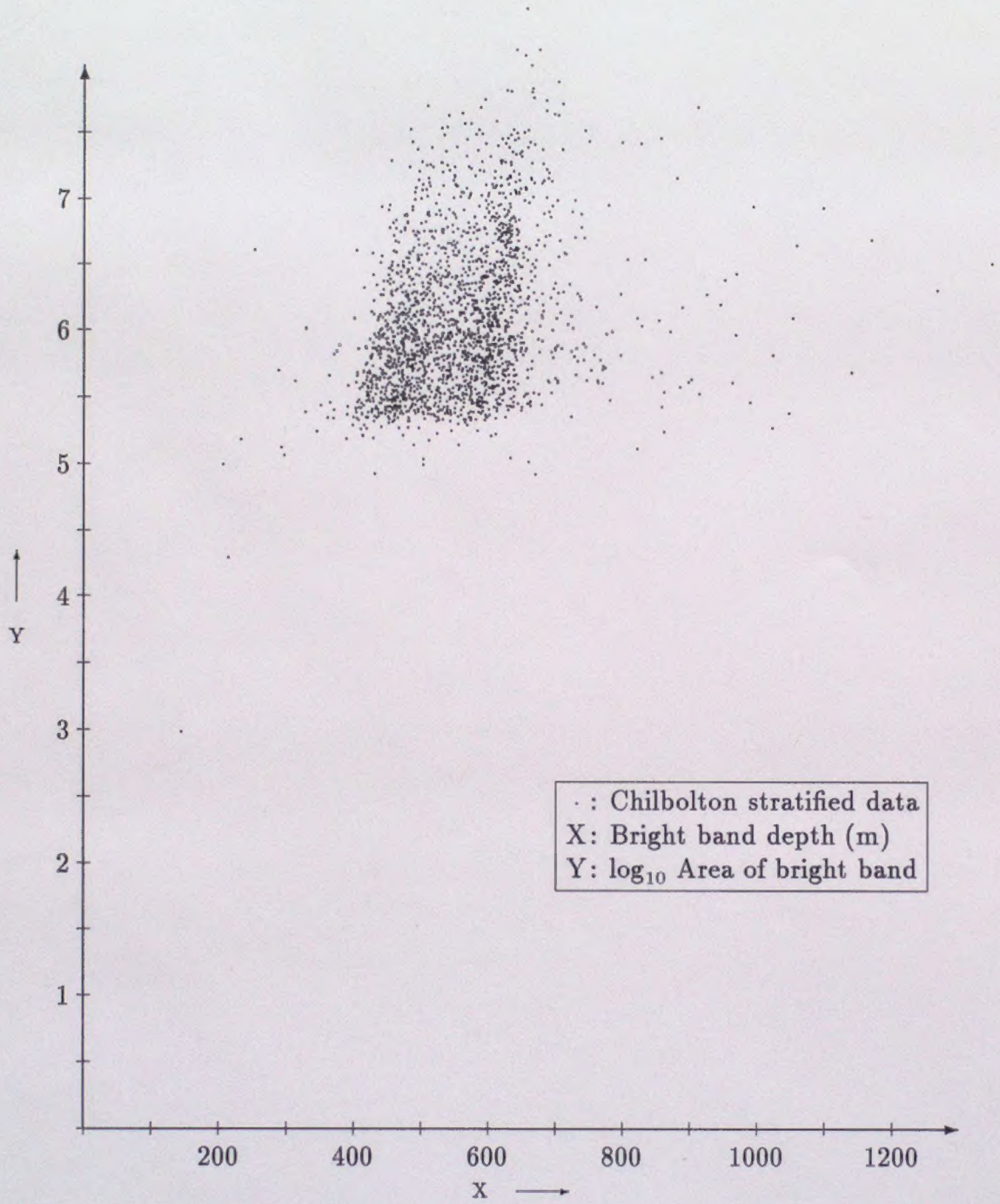

Figure 9

Area of bright band peak, from regression line $y = 1.045x + 2.300$, and depth. 2079 profiles used.

Short Range Forecasting Division Technical Reports

1.	ON THE TIME SAVING THAT CAN BE ACHIEVED BY THE USE OF AN OPTIMISED COURSE IN AN AREA OF VARIABLE FLOW	R.W. Lunnon A.D. Marklow September 1991
2.	Treatment of bias in satellite sea surface temperature observations	R.S.Bell August 1991
3.	FINITE DIFFERENCE METHODS	M.J.P. Cullen August 1991
4.	Representation and recognition of convective cells using an object-orientated approach	W.H. Hand 30th September 1991
5.	Sea-ice data for the operational global model.	C.P.Jones November 1991.
6.	Tuning and Performance of the Atmospheric Quality Control.	N.B. Ingleby. December 1991.
7.	More satellite sounding data - can we make good use of it?	R.S.Bell January 1992.
8.	WAM/UKMO Wind Wave model Intercomparison Summary Report	Heinz Gunther ECMWF Martin Holt UK Met Office January 1992
9.	Spin up problems of the UKMO Mesoscale Model and moisture nudging experiments	Akihide Segami JMA February 1992
10.	A comparison of 2nd generation and 3rd generation wave model physics	M.W. Holt B.J. Hall February 1992
11.	RETRIEVAL AND ASSIMILATION: SYSTEM CONSIDERATIONS	Andrew C Lorenc March 1992
12.	Detection of Precipitation by Radars in the UK Weather Radar Network	M. Kitchen P.M. Brown April 1992
13.	THE VALUE OF WIND OBSERVATIONS FOR WEATHER FORECASTING AND CLIMATE STUDIES	Andrew C Lorenc April 1992
14.	An investigation into the parameters used in the analysis scheme of the Mesoscale Model	G. Veitch B.J. Wright S.P Ballard May 1992
15.	THE VERIFICATION OF MESOSCALE MODEL FORECASTS OF LIQUID WATER CONTENT USING HELICOPTER REPORTS OVER THE NORTH SEA DURING WINTER 1991	M. Ahmed R.W Lunnon R.J. Graham May 1992

Short Range Forecasting Division Technical Reports

16.	Simulations of the Diurnal Evolution of Marine Stratocumulus Part I: The sensitivity of the Single Column Version of the Mesoscale Model to Changes in the Turbulence Scheme.	S.D.Jackson S.P. Ballard May 1992
17.	Simulations of the Diurnal Evolution of Marine Stratocumulus Part II: A Comparison of Radiation Schemes Using the Single Column Version of the Mesoscale Model.	S.D.Jackson S.P. Ballard May 1992
18.	Quantifying the low level windshear aviation hazard for the UK: some research proposals	R.J. Graham R.W. Lunnon May 1992
19.	WAM/UKMO Wind Wave model Intercomparison Part 2 Running the UKMO wave model at higher resolution	M.W. Holt April 1992
20.	Sensitivity of Mesoscale Model forecasts of anticyclonic Statocumulus to the specifications of initial conditions and Boundary Layer mixing scheme.	B.J. Wright S.P. Ballard July 1992
21.	Evaluation of diffusion and gravity wave changes in the Global Forecast Model.	F. Rawlins O. Hammon 16 June 1992
22.	Background Errors for the Quality Control and Assimilation of Atmospheric Observations in the Unified Model - the situation in July 1992.	C.A. Parrett July 1992
23.	Estimation of the Mean and Standard Deviation of the Random Component of Data also Containing Non- random Errors.	B.R. Barwell July 1992
24.	Experiments in Nowcasting convective rain using an object- oriented approach.	W.H. Hand 15th August 1992
25.	Gravity Wave Speeds from the Eigenmodes of the Unified	I. Roulstone 28 July 1992
26.	A re-calibration of the Wave Model	M.W. Holt August 1992
27.	Evaluation of Koistinen's method of radar range and bright band correction	A.G. Davies August 1992
28.	A Study of the Boundary Layer in the Mesoscale Unified Model	Graham Veitch August 21,1992
29.	Profiles of wind using time-sequences of absorption channel imagery from geostationary satellites: proof of concept using synthetic radiances	R.W.Lunnon September 1992
30.	AN EMPIRICAL INVESTIGATION OF THE "WATER VAPOUR TEMPERATURE LAPSE-RATE FEEDBACK" TO THE GREENHOUSE EFFECT	K.F.A. Smith R.J. Allam J.S.Foot September 1992
31.	Observation needs for operational ocean modelling	S.J. Foreman September 1992

Short Range Forecasting Division Technical Reports

32.	Bright band correlations for layered precipitation; the comparison of Chilbolton radar data and Hardaker model output.	A.G. Davies November 1992
33.	Progress and performance of the operational mesoscale model	S.P. Ballard
34.	Assessment of the bias of significant wave height in the Met.Office global wave model	S.J. Foreman M.W. Holt S. Kelsall